

000 001 002 003 004 005 006 007 008 009 010 011 012 013 014 015 016 017 018 019 020 021 022 023 024 025 026 027 028 029 030 031 032 033 034 035 036 037 038 039 040 041 042 043 044 045 046 047 048 049 050 051 052 053 GL-FUSION: RETHINKING THE COMBINATION OF GRAPH NEURAL NETWORK AND LARGE LANGUAGE MODEL

Anonymous authors

Paper under double-blind review

ABSTRACT

Recent research on integrating Large Language Models (LLMs) with Graph Neural Networks (GNNs) typically follows two approaches: LLM-centered models, which convert graph data into tokens for LLM processing, and GNN-centered models, which use LLMs to encode text features into node and edge representations for GNN input. LLM-centered models often struggle to capture graph structures effectively, while GNN-centered models compress variable-length textual data into fixed-size vectors, limiting their ability to understand complex semantics. Additionally, GNN-centered approaches require converting tasks into a uniform, manually-designed format, restricting them to classification tasks and preventing language output. To address these limitations, we introduce a new architecture that deeply integrates GNN with LLM, featuring three key innovations: (1) Structure-Aware Transformers, which incorporate GNN’s message-passing capabilities directly into LLM’s transformer layers, allowing simultaneous processing of textual and structural information and generating outputs from both GNN and LLM; (2) Graph-Text Cross-Attention, which processes full, uncompressed text from graph nodes and edges, ensuring complete semantic integration; and (3) GNN-LLM Twin Predictor, enabling LLM’s flexible autoregressive generation alongside GNN’s scalable one-pass prediction. GL-Fusion achieves outstanding performance on various tasks. Notably, it achieves state-of-the-art performance on OGBN-Arxiv and OGBG-Code2,

1 INTRODUCTION

Research in Graph Neural Networks (GNNs) has long focused on learning from graph with pre-processed vector features, often overlooking the rich textual information contained in raw data. Recently, many studies have recognized that better utilization of these text features can enhance performance. This has led to a focus on text-attributed graphs (TAGs), graphs with node, edge, and graph-level text attributes. In addition, some tasks may contain a task description, questions, and candidate answers in natural language. The combination of GNNs and pretrained Large Language Models (LLMs), which can efficiently encode these text attributes and information, has garnered significant interest.

Two main approaches have emerged for combining GNNs and LLMs: GNN-centered methods and LLM-centered methods. GNN-centered methods focus on typical graph tasks like node classification and link prediction. These methods convert text into representation vectors for graph nodes or edges using LLMs, which are then fed into GNNs to produce final predictions. GNN-centered approaches excel at capturing structural information. However, compressing rich textual features into fixed-length vectors results in information loss. Moreover, the importance of different text features varies depending on the task. For example, in wiki knowledge graph (KG) datasets, entity descriptions may include a person’s name, nationality, or occupation. A name might be crucial for identifying relatives but irrelevant for finding their workplace. Additionally, GNN architectures cannot generate natural language, making it difficult to perform tasks like question answering.

LLM-centered methods, on the other hand, use a multi-modal approach by projecting graph representations into the language space, allowing LLMs to generate text answers to graph-text questions.

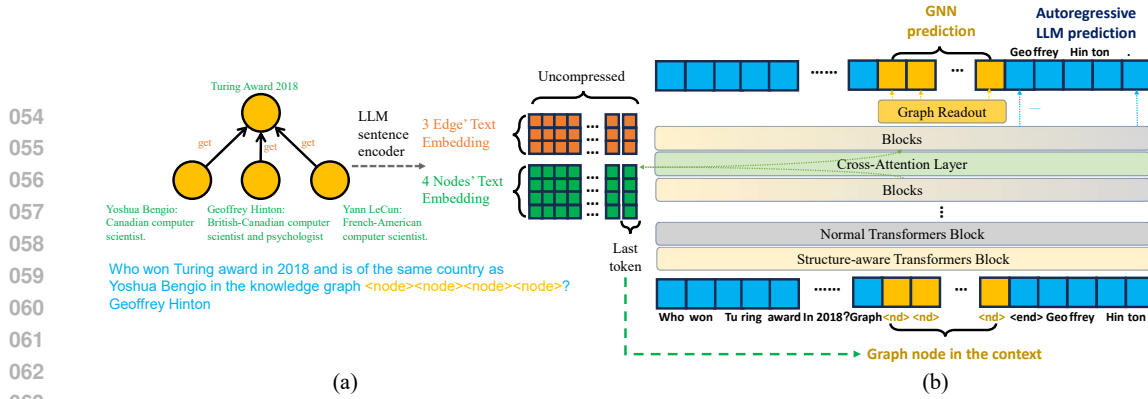


Figure 1: Workflow of the GL-Fusion model. (a) An example of a text-attributed graph, where each node and edge has a text attribute that will be encoded by the LLM. (b) The encoded text-attributed graph nodes ($<\text{node}>$ in the figure), along with a prompt or question in natural language, are merged into an input sequence for our GL-Fusion model. GL-Fusion consists of several structure-aware transformer blocks and standard transformer blocks. Cross-attention layers are inserted to retrieve the complete, uncompressed node and edge text. The output on graph nodes is further processed by graph readout components, while the output on standard text tokens predicts the next token, similar to an original autoregressive LLM.

However, this approach faces similar challenges. Graph tasks vary widely in domains, and current LLM-centered models lack dynamic encoding by GNNs that adapt to tasks, so these models struggle to generalize to diverse datasets or tasks. Furthermore, language supervision is often indirect and less efficient compared to direct graph supervision, making training more difficult. For example, LLMs, with their autoregressive nature, cannot simultaneously predict all nodes in a graph, unlike GNNs, which can process nodes in parallel. Moreover, GNNs focus on classifying nodes into a finite set of classes, while LLMs operate in the much larger and noisier token space of natural language, complicating the training process.

To handle tasks involving both graphs and text, we introduce Graph-Language Fusion (GL-Fusion), an architecture that combines the strengths of GNN-centered and LLM-centered models. As shown in Figure 1(a), graphs are paired with node and edge text features to solve tasks described in natural language. In Figure 1(b), the task description is included as part of the input text sequence, and a special token $<\text{node}>$ is added for each graph node. Each node's feature is generated by a text encoder based on its text attribute, which is then incorporated into the sequence. To process this combination of graph and text tokens, our architecture includes:

- **Structure-Aware Transformer Layers:** We modify the original attention layers for language input to graph structure-aware attention with both graph and text inputs, which maintains causality for language generation and further enabling transformer to encode graph structure. Different from graph transformer, which encodes graph only and cannot process text, our transformer can naturally encode graph tokens conditioning on the text tokens before it in sequence, and encodes text tokens after the graph based on the graph. This two-way information exchange between graph and text overcomes the limitations of older models, where either graph or text embedding is irrelevant from the other, and achieves better expressivity.
- **Graph-Text Cross-Attention:** Previous models often compress either graph or text information into a single vector, leading to information loss. In our model, graph structure is preserved across each transformer layer without compression. To avoid compressing textual features, we introduce Graph-Text Cross-Attention layers, where attention is applied between node text and the main sequence (which includes the $<\text{node}>$ tokens). These layers retain the complete text information of each node, allowing the model to more precisely extract task-relevant information by focusing on the most important tokens.
- **GNN & LLM Twin-Predictor:** Different tasks require different prediction mechanisms. For traditional GNN tasks, such as node classification, having the LLM generate predictions for each node would slow down inference and be constrained by graph size. In such cases, direct readout from the GNN is more efficient. Conversely, tasks that require natural language outputs benefit from the autoregressive capabilities of LLMs. Unlike previous models, which rely on either a GNN or LLM predictor, GL-Fusion retains both as predictors. During training, supervision can be applied to both models, and during inference, both outputs are generated simultaneously. Users can choose the most appropriate output for the task or consider both outputs together.

108 With these modifications, we propose GL-Fusion, a unified architecture that achieves competitive
 109 performance by integrating structural and textual information. To demonstrate this, we conducted
 110 experiments on various tasks, including basic graph property prediction, node classification, knowl-
 111 edge graph completion, commonsense question answering, and code graph-to-text generation. Our
 112 GL-Fusion achieves outstanding performance across all these datasets, outperforming various com-
 113 binations of GNNs and LLMs. Notably, our model even achieves state-of-the-art performance on
 114 two Open Graph Benchmark (Hu et al., 2020) datasets: ogbn-arxiv and ogbg-code2. These results
 115 demonstrate the powerful capability of our GL-Fusion architecture.

116

117 2 PRELIMINARY

118

119 For a tensor $Z \in \mathbb{R}^{a \times b}$, let $Z_i \in \mathbb{R}^b$ denote the i -th row, $Z_{:,j} \in \mathbb{R}^a$ denote the j -th column, and
 120 $Z_{ij} \in \mathbb{R}$ denote the element at the (i, j) -th position.

121

122 **Text-Attributed Graph (TAG)** A TAG is represented as $\mathcal{G} = (V, E, X)$, where $V =$
 123 $1, 2, 3, \dots, n$ is the set of n nodes, $E \subseteq V \times V \times \mathcal{Z}^{L_e}$ is the set of edges. Each edge $(i, j, E_{ij}) \in E$
 124 connects node i and node j with text E_{ij} consisting of L_e tokens. The node text feature matrix is
 125 denoted as $X \in \mathbb{Z}^{n \times L_n}$, where X_i represents the L_n -token text feature of node i . Here, L_n and
 126 L_e represent the maximum lengths of node and edge text, respectively. Text of varying lengths is
 127 padded to the same length.

128

129 **Problem Settings** We consider a TAG \mathcal{G} and a task description $T \in \mathcal{Z}^{L_t}$. The task can be node
 130 classification, link prediction, graph classification, or text generation. As illustrated in Figure 1,
 131 our model processes a TAG along with a task description. The graph is integrated into the task
 132 description as part of the input sequence to our model, where the graph forms a subsequence starting
 133 with a special `<graph_start>` token and ending with a `<graph_end>` token. Each node is
 134 represented by a `<node>` token. For each specific task, we use a task-specific prediction head,
 135 and the model also leverages the LLM itself to generate the answer in text form. We focus on
 136 the supervised learning setting, where the dataset is split into training, validation, and test sets.
 137 Models are trained on the training set, hyperparameters are tuned on the validation set, and test set
 138 performance is reported.

139

140 3 GL-FUSION: A HIGHLY INTEGRATED GNN-LLM MODEL

141

142 This section presents the architecture of our GL-Fusion model, which integrates structure-aware
 143 transformer layers, graph-text cross-attention blocks, and GNN & LLM twin predictors. Given input
 144 sequence $T \in \mathbb{Z}^{L_t}$ and input graph $\mathcal{G} = (V, E, X)$, we first convert T to sequence representation
 145 $t \in \mathbb{R}^{L_t \times d}$ with token embedding layer. Then we use an existing text encoder (BehnamGhader et al.,
 146 2024) to convert node text sequences X to uncompressed text embeddings $x \in \mathbb{R}^{n \times L_n \times d}$, and we
 147 also convert edge text $E_{ij} \in \mathbb{Z}^{L_e}$ to compressed text embedding $e_{ij} \in \mathbb{R}^d$. Our GL-Fusion model
 148 will update input sequence representations t in each transformer layer and use t to produce the final
 149 prediction.

150

151 3.1 STRUCTURE-AWARE TRANSFORMER LAYER

152

153 To encode the input sequence, a mixture of text and node tokens, we propose a structure-aware
 154 transformer layer that fulfills the following properties: (1) Preserving causality for text generation.
 155 (2) Maintaining invariance to node permutation. (3) Encoding edges between nodes. Figure 2a
 156 illustrates this structure-aware architecture. Compared to ordinary transformer layers, it includes the
 157 following extensions.

158

159 **Graph-aware attention mask and positional encodings** To preserve causality for text genera-
 160 tion, a causal mask keeps only the lower triangle of the attention matrix, setting all other entries to
 161 zero. In other words, each token can only aggregate embeddings from previous tokens, prohibiting
 162 the use of representations from tokens that come after it. While directly applying the causal mask
 163 to the mixed sequence preserves causality for text generation, it disrupts permutation equivariance;
 164 that is, each graph token can only aggregate information from graph tokens preceding it, making the

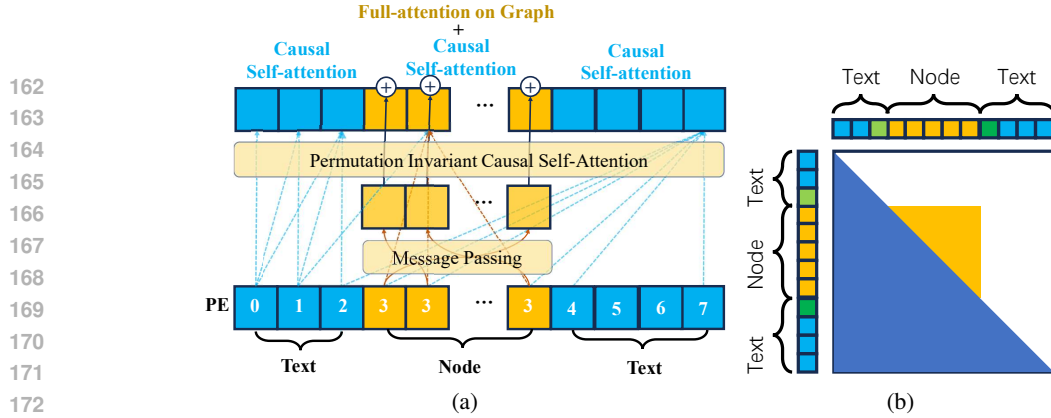


Figure 2: Design of Structure-Aware Transformer layer. (a) Structure-aware Transformer layer. The brown curve indicates the message-passing process along graph edges. The dashed brown and blue lines represent causal self-attention and full attention, respectively. The boxed numbers indicate shared positional encodings. (b) The attention mask in structure-aware transformer layers. The blue part represents the ordinary causal attention mask, and the yellow part allows attention between nodes in the same graph.

order of graph tokens affect the output. This violates the permutation invariance of node indices, which is crucial for graph learning.

To address this, we propose the following attention masks. All tokens can aggregate information from any token before them. However, for node tokens, other node tokens within the same graph are also visible to them, preserving permutation invariance. Additionally, causality for text generation is maintained as graph tokens are not generated. Furthermore, to preserve causality, we only allow graph tokens to attend to text tokens that come before them, and text tokens can only attend to graph tokens that come before them. The resulting attention mask is shown in Figure 2b.

To further ensure permutation invariance, we assign the same positional encodings to all node tokens in the same graph as the corresponding `<graph_start>` token. Additionally, all graph tokens use a single index, as shown in the positional encoding (PE) of Figure 2a, preventing the model from running out of the context window for large graphs.

Message Passing with Multiple Aggregators. To encode graph structure, we involve a message passing layer (Gilmer et al., 2017) in our transformer layer. Our message-passing layer updates the representation of node u as follows:

$$h'_u = \text{COMBINE}(h_u, \text{AGGREGATE}(\{h_v \odot e_{uv} | v \in N(u)\})), \quad (1)$$

where $h_u \in \mathbb{R}^d$ is the representation of node u , produced by a linear layer with the corresponding node token representation t_i , $e_{uv} \in \mathbb{R}^d$ is the edge feature extracted from text, and $N(u)$ denotes neighboring nodes. Following Corso et al. (2020), we employ three aggregators: mean, max, and std, concatenating their outputs into a \mathbb{R}^{3d} vector, which is then projected back to $h'_u \in \mathbb{R}^d$ via a linear layer.

To manage the varying importance of graph structure information across tasks, we introduce a gating mechanism. The gate value is computed with a linear layer and a tanh activation function with the original token embedding as input, updating t_i , the representation of node token i , corresponding to node u as:

$$t_i \leftarrow t_i + \tanh(W t_i) h_u, \quad (2)$$

where $W \in \mathbb{R}^{1 \times d}$. All elements in W are initialized as 0 and optimized in the training process. So the gate value and thus the output of Message Passing module is 0 initially. This mechanism allows gradual integration of GNN outputs during training while stabilizing the model and mitigating knowledge forgetting.

3.2 GRAPH-TEXT CROSS-ATTENTION

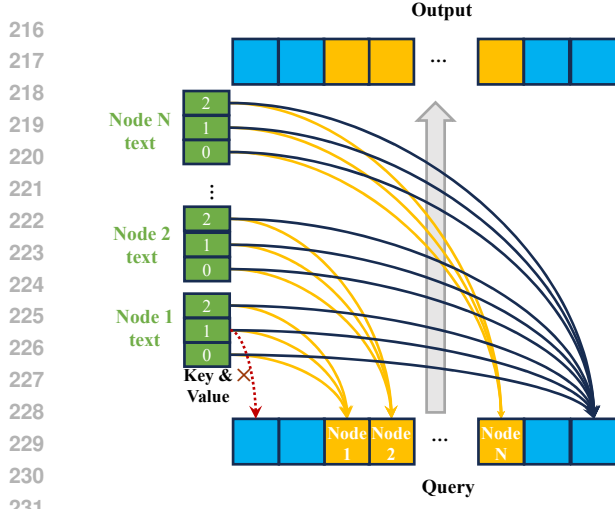


Figure 3: The attention mask in cross-attention layers. For text tokens before the graph, they do not involve cross-attention to maintain causality (red dashed line with the \times). For node tokens $\langle \text{node} \rangle$, each token only has access to its own text (orange lines). For text tokens after the graph, they have access to all node text (black lines).

One significant drawback of previous GNN-centered models is that they compress node, edge text features, and task descriptions into fixed-size representations, while LLM-centered methods tend to compress graph structure into fixed-size representations, leading to significant information loss. With our structure-aware transformer layer, we encode the graph structure and task description directly in each layer without compression. To avoid compression of node/edge text features, we introduce the Graph-Text Cross-Attention block to enable node token representations and text tokens generated after the node token to extract information from the raw node text. Note that we can also use the cross-attention block to extract information from edge text. However, most datasets currently have simple and unvaried edge features, so we primarily focus on extracting information from raw node text.

The architecture is shown in Figure 3. The cross-attention block extracts features from the node text representation x to update the task representation t as follows.

To update t_i , the representation of token i , first, each node’s text representation of L_n tokens is aggregated into a single representation. For node v ,

$$x'_{iv} = \text{softmax} \left(\frac{1}{\sqrt{d}} t_i^T W_{Q1}^T W_{K1} x_v^T \right) x_v \in \mathbb{R}^d, \quad (3)$$

where $t_i \in \mathbb{R}^d$ is the query of cross attention, $W_{Q1}, W_{K1} \in \mathbb{R}^{d \times d}$ are learnable linear layer for query and key, and $x_v \in \mathbb{R}^{L_n \times d}$ is the uncompressed text representation of node v . x'_{iv} is the feature extract from node v for updating token i ’s representation. Then, all nodes’ features are further aggregated:

$$t'_i = \begin{cases} x'_{iv} & \text{if } i \text{ is the node token w.r.t. node } v, \\ \text{softmax}(t_i^T W_{Q2}^T W_{K2} x'_{iv}) x'_{iv} & \text{if } i \text{ is a text token,} \end{cases} \quad (4)$$

where \mathbf{v} is the set of nodes whose token in input sequence is before i , $x'_{iv} \in \mathbb{R}^{|\mathbf{v}| \times d}$ is the sequence of x'_{iv} for node v in \mathbf{v} , and $W_{Q2}, W_{K2} \in \mathbb{R}^{d \times d}$ are learnable linear layers. Then $t'_i \in \mathbb{R}^d$ is used to update t_i . To maintain causality, we only allow text tokens to aggregate features from graph nodes preceding them in the input sequence. For text tokens, if there is no graph token before, the resulting cross-attention result is 0. For node tokens, although they can aggregate text features from other nodes, in experiments we find that this may cause all nodes to have similar representations, which makes them indistinguishable from each other. Therefore, we constrain each node to extract information solely from its own text to avoid this problem.

Compared to the cross-attention block, directly adding node text to the input sequence of the LLM may seem more straightforward. However, it introduces several challenges. First, it is difficult to design a special positional encoding (PE) and attention mask that preserve causality for text and permutation invariance for graphs in the structure-aware layer. Second, in terms of computational complexity, the naive text-in-context method incurs $O((nL_n + L_t)^2)$ time complexity as $n L_n$ -length node text sequences are added to the context window. In contrast, our cross-attention method simplifies the complexity to $O(nL_n \cdot L_t)$, significantly reducing costs and enabling our model to handle larger graphs efficiently, as is often the case when $nL_n \gg L_t$.

3.3 GNN & LLM TWIN PREDICTOR

Since our model uses a transformer architecture and maintains causality, it can naturally generate text outputs, which we refer to as the LLM predictor. Additionally, since graph nodes are treated

270 as tokens in the input sequence, the transformer’s output representations for these tokens can be
 271 considered node-level GNN representations, which can be fed into pooling layers and linear layers
 272 to produce predictions—referred to as the GNN predictor. Both predictors have their advantages
 273 and disadvantages, as outlined below:

275 **Rationale for GNN as a Predictor.** While LLMs can perform various language tasks, they face
 276 limitations in autoregressive generation, including:

- 277 • **Natural Language Output:** LLMs can natively produce text predictions, which is challenging for
 278 the GNN predictor.
- 279 • **Numerical Output:** GNN predictors naturally output numerical values, making them well-suited
 280 for regression or ranking tasks. In contrast, LLMs produce token sequences, making it difficult to
 281 generate numerical outputs as text.
- 282 • **Scalability:** LLMs predict outputs one by one in an autoregressive manner, which can be ineffi-
 283 cient for tasks requiring multiple predictions for all nodes or edges. In contrast, GNNs generate
 284 all predictions for all nodes or edges in parallel.
- 285 • **Training Efficiency:** Training models end-to-end through LLM-generated sequences is more in-
 286 direct and harder to control, as the LLM’s loss function is constrained by “perplexity” (i.e., the
 287 cross-entropy loss on token space), which often includes task-irrelevant tokens instead of focus-
 288 ing solely on the task-relevant labeling space. With GNNs, we can provide direct and dense
 289 supervision on the target classes, improving training efficiency.

290 To leverage both approaches, we employ a twin-predictor architecture, allowing for simultaneous
 291 predictions from both the GNN and LLM. A graph readout component, tailored to specific tasks, is
 292 added after the final layer for GNN predictions. This component is trained using cross-entropy loss
 293 for classification tasks or mean squared error for regression tasks. During inference, it can generate
 294 predictions for graph nodes as needed.

296 4 RELATED WORK

297 **LLM-Centered Approaches** LLM-centered methods leverage pretrained language models to
 298 handle graph data by translating graph structures into text formats, like adjacency lists (Liu & Wu,
 299 2023; Guo et al., 2023b; Chen et al., 2024). While these methods have shown some promise, they
 300 often suffer from issues related to node and edge ordering and can struggle with large graphs due
 301 to the limited context windows of LLMs. A more effective solution has been to use GNNs to gen-
 302 erate node representation sequences that are fed into LLMs. For example, Chai et al. (2023) used
 303 embeddings from Message Passing Neural Networks (MPNNs) to represent target nodes, enabling
 304 the LLM to answer basic structural questions. Similarly, Tang et al. (2024) aligned both structural
 305 and textual inputs using GNNs and Transformers, achieving better accuracy by processing all node
 306 embeddings through a frozen pretrained LLM. However, these approaches can still face limitations,
 307 such as task-agnostic encoders, as seen in Qin et al. (2024), which limit their ability to transfer
 308 across different domains.

309 **GNN-Centered Approaches** In GNN-centered methods, LLMs are primarily used to encode tex-
 310 tual data that is then fed into GNNs for tasks like node classification and link prediction. Early
 311 graph datasets such as Cora (McCallum et al., 2000) and CiteSeer (Giles et al., 1998) used basic text
 312 embeddings, but these often failed to capture complex textual information. More recent datasets,
 313 like OGB-WikiKG90Mv2 (Hu et al., 2021), have improved this by utilizing pretrained sequence en-
 314 coders. Duan et al. (2023) demonstrated that fine-tuning LLMs before passing textual information
 315 to GNNs significantly boosts performance. Further work by Ioannidis et al. (2022) and Xie et al.
 316 (2023) introduced novel fine-tuning strategies to better integrate LLMs into GNN tasks. Besides,
 317 with many powerful LLMs being closed-source, researchers like He et al. (2024) have proposed aug-
 318 menting graph data with enhanced text features generated by accessible LLMs. While they improve
 319 performance, these models like OFA (Liu et al., 2023) still compress textual data into fixed-length
 320 vectors, limiting their application to tasks with complex text features.

321 **GNN-LLM Fusion** Recent efforts aim for a deeper integration of GNNs and LLMs. One exam-
 322 ple is GraphFormers (Yang et al., 2023), which proposed an architecture that combines GNNs and

324 Table 1: Results in accuracy (%) on Basic Graph Property Prediction Tasks.
325

	GL-Fusion	EdgePrompt	GML	GraphML	w/o Cross Atten
degree	100	44.87	20.91	40.20	100
edge	99.78	74.60	50.45	62.05	100
node text	34.50	-	-	-	0.00

331 Table 2: Results in accuracy (%) on node classification Tasks.
332

	GL-Fusion	GLEM	XRT	OneForAll	GPT4graph	GraphGPT	GCN
Ogbn-arxiv	78.20	76.12	76.94	77.51	60.00	75.11	71.47
Cora	84.3	-	-	74.76	-	-	81.5

338 Transformers by iteratively encoding text and aggregating graph structures across layers. While this
339 approach improves text encoding for graph nodes, it overlooks the inclusion of task descriptions or
340 language prompts. Furthermore, the lack of autoregressive generation and cross-attention mechan-
341 isms restricts the model’s ability to dynamically extract task-specific information. Building on this,
342 Jin et al. (2023) adapted the GraphFormers architecture by refining its pretraining strategy, aiming
343 to better capture text relationships between neighboring nodes. While these methods have made
344 strides, there is still a need for more tightly integrated approaches that can fully exploit the potential
345 of GNNs and LLMs working together.

346

5 EXPERIMENTS

347 To evaluate the potential of GL-Fusion as a new architecture combining GNN and LLM, we con-
348 ducted experiments on various tasks. These include synthetic tasks to validate its capacity to capture
349 basic graph properties, traditional GNN tasks such as node classification and link prediction to as-
350 sess its ability to solve graph-related tasks, commonsense question-answering tasks to test its ability
351 to leverage knowledge graphs for language generation, and code graph tasks to evaluate its capacity
352 to generate text based on graph structures. Through these experiments, we demonstrate GL-Fusion’s
353 strong potential to effectively combine GNN and LLM architectures. Further details on the experi-
354 ments can be found in Appendix A.

355

5.1 BASIC GRAPH PROPERTY PREDICTION

356 Following Guo et al. (2023a), we evaluate our model on basic graph property prediction tasks. We
357 consider two tasks: degree (to predict a node’s degree with the whole graph as input) and edge (to
358 predict whether there exists an edge between two nodes in the graph). These two properties are
359 simple for GNN-centered methods. However, for LLM-centered methods, graph structural features
360 are often compressed and thus incomplete, leading to difficulties. The baselines include LLM-
361 centered methods such as EdgePrompt, GML, and GraphML from Guo et al. (2023a). We also
362 conduct an ablation study on these two tasks. Additionally, we introduce a node text retrieval task,
363 where models attempt to predict the input sentence of a node. The results are shown in Table 1. In
364 general, GL-Fusion outperforms all these baselines and captures basic graph properties perfectly.
365 Moreover, GL-Fusion without cross-attention results in significantly lower precision on the node
366 text task, validating the effectiveness of our cross-attention block in extracting information from
367 node text.

368

5.2 NODE CLASSIFICATION

369 We demonstrate our model’s ability to leverage both textual features and graph structure in TAG
370 through a node classification task. We evaluate GL-Fusion on two datasets: ogbn-arxiv (Hu et al.,
371 2020) and Cora (Yang et al., 2016). The baselines include GCN (Kipf & Welling, 2017), the GNN-
372 centered model GLEM (Zhao et al., 2023), XRT (Chien et al., 2022), OFA (Liu et al., 2023), and
373 the LLM-centered methods GPT4graph (Guo et al., 2023a), MuseGraph (Tan et al., 2024), and
374 GraphGPT (Tang et al., 2024). The results are shown in Table 2. We also conduct experiments in

378 Table 3: Results in test accuracy(%) on ogbn-arxiv dataset with a few training samples.
379

#shots	Feature	PLM+GAE	GIANT	PLM-cls	PLM-dense	PLM-sparse	G-Prompt	GL-Fusion
10	45.76	51.89	51.4	46.97	51.17	52.01	52.48	56.44
100	58.75	60.63	61.26	58.69	58.65	60.85	61.67	68.18

384 Table 4: Node classification on CSTAG datasets (Yan et al., 2023). Sports uses F1 score. Other
385 datasets use accuracy.
386

Model	GL-Fusion	PLM-Based			GNN-Based			Co-Training Based	
		Tiny	Base	T-GCN	B-GCN	T-SAGE	B-SAGE	GCN(T)	SAGE(T)
Children	61.19	49.85	59.91	57.07	58.11	57.57	58.74	54.75	59.7
History	86.16	83.06	86.09	84.52	85.04	84.79	85.12	83.52	85.09
Photo	82.89	73.75	77.53	82.42	82.7	83.25	83.27	83.32	86.64
Computers	88.91	58.32	60.4	87.43	87.86	87.9	88.3	83.93	86.04
Sports	93.33	81.47	86.02	84.93	86.16	87.06	87.34	85.06	85.87

397 few-shot settings following (Huang et al., 2023). The results are shown in Table 3. #shot means
398 the number of training set per class. Baselines are from Huang et al. (2023). Our model outper-
399 forms existing models significantly. Besides these datasets, we also conduct experiments on CSTAG
400 benchmark (Yan et al., 2023). We use the datasets and baseline in (Yan et al., 2023). PLM-Based
401 models uses LLM to encode target node text only. GNN-Based methods uses GNN to encode graph
402 with node feature provided by fixed LLM. Co-Training methods denote methods training GNN and
403 LLM simultaneously. The results are shown in Table 4. Our GL-Fusion significantly outperforms
404 all baselines on most datasets, verifying the model’s capacity for ordinary graph tasks.

406 5.3 KNOWLEDGE GRAPH COMPLETION

408 We demonstrate our model’s ability to leverage both textual and structural information through the
409 knowledge graph completion task, using the Wikidata Knowledge Graph, which provides rich tex-
410 tual descriptions and structural relationships. We employ the FB15k-237-ind dataset (Teru et al.,
411 2020), extracted from Freebase (Bollacker et al., 2008), featuring four standard training and test
412 splits with shared relation types but disjoint entities. Each node and edge is annotated with textual
413 attributes: entities include names and brief descriptions, while edges retain their textual represen-
414 tations from Freebase. Following approaches like NBFNet (Zhu et al., 2022) and UniLP (Mikhail
415 et al., 2024), we annotate nodes with distances to their corresponding head or tail nodes for predic-
416 tion tasks.

417 For baselines, we select several representative inductive learning GNNs and KG-BERT (Yao et al.,
418 2019) for LLM-based completion. Recent methods using LLMs for KG completion, such as few-
419 shot prompting (BertRL)(Zha et al., 2021) or explicit rule learning (KRST)(Su et al., 2023), are
420 also included as they focus on different techniques. Our results, shown in Table 5, indicate that
421 our model outperforms all baselines across the four splits, effectively utilizing both linguistic and
422 structural information.

423 5.4 COMMON SENSE QUESTION ANSWERING

425 CommonsenseQA (Talmor et al.) is a 5-way multiple choice Question Answering task that requires
426 reasoning with commonsense knowledge, containing 12,102 questions. It can be solved with an
427 pure language model. However, following (Yasunaga et al., 2021). for each problem, we sample a
428 subgraph containing entities in the problem from a knowledge graph. Our baselines include com-
429 bination of Knowledge graph and LLM: , QAGNN (Yasunaga et al., 2021) and some pure LLM
430 results from (Xu et al., 2021). The results are shown in Table 6. Note that our GL-Fusion is base on
431 Llama3-8b, and our model outperforms Llama3-8b with prompt significantly, verifying that learning
on KG indeed significantly boost model’s performance.

Table 5: Inductive link prediction on FB15k237-ind dataset. Higher scores are better. KG-BERT serves as a baseline LLM, while others are GNNs. KG-BERT performance is from Zha et al. (2021); GNN baselines are from Zhu et al. (2024).

Method	MRR	v1		v2		v3		v4	
		H@1	H@10	MRR	H@1	H@10	MRR	H@1	H@10
GraIL	0.443	0.329	0.642	0.614	0.495	0.818	0.642	0.531	0.828
NBFNet	0.625	0.519	0.834	0.769	0.673	0.949	0.762	0.668	0.951
UniLP	0.754	0.672	0.921	0.808	0.734	0.943	0.793	0.720	0.945
KG-BERT	0.500	0.341	-	-	-	-	-	-	-
BertRL	0.605	0.541	-	-	-	-	-	-	-
KRST	0.716	0.602	-	-	-	-	-	-	-
GL-Fusion	0.8558	0.7306	0.9830	0.8558	0.7761	0.9853	0.8257	0.7379	0.9861

Table 6: Result in accuracy (%) in CommonsenseQA tasks.

Model	GL-Fusion	QA-GNN	GPT-3 Finetuned	Llama3-8b
ACC	81.79	76.1	73.0	59.4

Table 7: Function name generation task on ogbg-code2 dataset. Baseline results are from the OGB (Hu et al., 2020) leaderboard.

Model	GAT	GraphTrans	SAT++	DAGformer	GL-Fusion
Test F1(%)	15.69 ± 0.10	18.30 ± 0.24	22.22 ± 0.32	20.18 ± 0.21	40.97

Table 8: Ablation study on ogbn-arxiv dataset. All results are text accuracy (\uparrow)

	Original	Low Rank	w/o cross atten	w/o gate	w/o aggrs	w/o gnn pred	w/o text pred
GNN	77.09	76.61	75.5	75.88	75.4	-	75.8
LLM	76.43	75.97	74.97	73.33	75.57	72.45	-
Ensemble	78.2	77.06	76.35	76.2	76.48	-	-

5.5 GRAPH-TO-LANGUAGE GENERATION

While image-to-text and video-to-text generation are well-studied, graph-to-language generation remains underexplored. We evaluate our GL-Fusion model on the ogbg-code2 dataset (Hu et al., 2020), where each graph represents the Abstract Syntax Tree (AST) of a Python function, and the goal is to predict the function name from the AST. Previous methods have treated this as a classification task, assuming uniform function name lengths and a limited token set, which is impractical. In contrast, our model generates text directly. The results are shown in Table 6. Our GL-Fusion model outperforms state-of-the-art methods (Velickovic et al., 2018; Luo et al., 2023) significantly, verifying the strong potential of our architecture.

5.6 ABLATION STUDY

To verify the effectiveness of our designations, we conduct ablation study on ogbn-arxiv dataset. The results are shown in Table 8. In the table, Low rank denotes using model with LoRA rank=8. w/o cross atten removes the graph-text cross attention. w/o gate removes the gate mechanism. w/o aggrs removes multiple aggregators in the message passing modules in transformer layers and uses mean aggregator only. w/o gnn pred removes the gnn prediction and training loss on it. w/o text pred removes the text prediction and training loss on it. Each module contributes to the overall performance, and removing any of them results in a performance drop.

6 CONCLUSION

This paper addresses key challenges in integrating GNNs and LLMs, such as independent encoding of text and structure, task-agnostic text representation, excessive information compression, and issues with output scalability and flexibility. We propose the GL-Fusion architecture, featuring three innovations: 1. Integrated Structural and Textual Learning by combining MPNNs with self-attention layers; 2. Graph-text cross-attention modules that preserve full textual content to prevent information loss; and 3. A GNN-LLM twin-predictor that facilitates predictions as both LLM and GNN for enhanced scalability and flexibility. Our experiments on the various datasets demonstrate that GL-Fusion effectively leverages language and structure, significantly improving reasoning performance in graph-text tasks.

486 **LLM USAGE**
487488 We use the LLM to polish our writing and check our grammar over the full paper.
489490 **REFERENCES**
491492 Parishad BehnamGhader, Vaibhav Adlakha, Marius Mosbach, Dzmitry Bahdanau, Nicolas Cha-
493 pados, and Siva Reddy. Llm2vec: Large language models are secretly powerful text encoders.
494 *CoRR*, abs/2404.05961, 2024.495 Kurt Bollacker, Colin Evans, Praveen Paritosh, Tim Sturge, and Jamie Taylor. Freebase: a collab-
496 oratively created graph database for structuring human knowledge. In *Proceedings of the 2008*
497 *ACM SIGMOD International Conference on Management of Data*, SIGMOD '08, pp. 1247–1250,
498 New York, NY, USA, 2008. Association for Computing Machinery. ISBN 9781605581026. doi:
499 10.1145/1376616.1376746. URL <https://doi.org/10.1145/1376616.1376746>.500 Ziwei Chai, Tianjie Zhang, Liang Wu, Kaiqiao Han, Xiaohai Hu, Xuanwen Huang, and Yang Yang.
501 Graphllm: Boosting graph reasoning ability of large language model, 2023.502 Zhikai Chen, Haitao Mao, Hang Li, Wei Jin, Hongzhi Wen, Xiaochi Wei, Shuaiqiang Wang, Dawei
503 Yin, Wenqi Fan, Hui Liu, and Jiliang Tang. Exploring the potential of large language models
504 (llms) in learning on graphs, 2024.505 Eli Chien, Wei-Cheng Chang, Cho-Jui Hsieh, Hsiang-Fu Yu, Jiong Zhang, Olgica Milenkovic, and
506 Inderjit S. Dhillon. Node feature extraction by self-supervised multi-scale neighborhood predic-
507 tion. In *ICLR*, 2022.508 Gabriele Corso, Luca Cavalleri, Dominique Beaini, Pietro Liò, and Petar Velickovic. Principal
509 neighbourhood aggregation for graph nets. In *NeurIPS*, 2020.510 Keyu Duan, Qian Liu, Tat-Seng Chua, Shuicheng Yan, Wei Tsang Ooi, Qizhe Xie, and Junxian He.
511 Simteg: A frustratingly simple approach improves textual graph learning, 2023.512 Matthias Fey and Jan Eric Lenssen. Fast graph representation learning with pytorch geometric.
513 *arXiv preprint arXiv:1903.02428*, 2019.514 C. Lee Giles, Kurt D. Bollacker, and Steve Lawrence. Citeseer: an automatic citation indexing
515 system. In *Proceedings of the Third ACM Conference on Digital Libraries*, DL '98, pp. 89–98,
516 New York, NY, USA, 1998. Association for Computing Machinery. ISBN 0897919653. doi:
517 10.1145/276675.276685. URL <https://doi.org/10.1145/276675.276685>.518 Justin Gilmer, Samuel S Schoenholz, Patrick F Riley, Oriol Vinyals, and George E Dahl. Neural
519 message passing for quantum chemistry. In *ICML*, pp. 1263–1272, 2017.520 Jiayan Guo, Lun Du, and Hengyu Liu. Gpt4graph: Can large language models understand graph
521 structured data? an empirical evaluation and benchmarking. *CoRR*, abs/2305.15066, 2023a.522 Jiayan Guo, Lun Du, Hengyu Liu, Mengyu Zhou, Xinyi He, and Shi Han. Gpt4graph: Can large
523 language models understand graph structured data ? an empirical evaluation and benchmarking,
524 2023b.525 Xiaoxin He, Xavier Bresson, Thomas Laurent, Adam Perold, Yann LeCun, and Bryan Hooi. Har-
526 nessing explanations: Llm-to-lm interpreter for enhanced text-attributed graph representation
527 learning, 2024.528 Weihua Hu, Matthias Fey, Marinka Zitnik, Yuxiao Dong, Hongyu Ren, Bowen Liu, Michele Catasta,
529 and Jure Leskovec. Open graph benchmark: Datasets for machine learning on graphs. In *NeurIPS*,
530 2020.531 Weihua Hu, Matthias Fey, Hongyu Ren, Maho Nakata, Yuxiao Dong, and Jure Leskovec. Ogb-lsc:
532 A large-scale challenge for machine learning on graphs. *arXiv preprint arXiv:2103.09430*, 2021.

540 Xuanwen Huang, Kaiqiao Han, Dezheng Bao, Quanjin Tao, Zhisheng Zhang, Yang Yang, and
 541 Qi Zhu. Prompt-based node feature extractor for few-shot learning on text-attributed graphs.
 542 *CoRR*, abs/2309.02848, 2023.

543 Vassilis N. Ioannidis, Xiang Song, Da Zheng, Houyu Zhang, Jun Ma, Yi Xu, Belinda Zeng, Trishul
 544 Chilimbi, and George Karypis. Efficient and effective training of language and graph neural
 545 network models, 2022.

546 Bowen Jin, Wentao Zhang, Yu Zhang, Yu Meng, Xinyang Zhang, Qi Zhu, and Jiawei Han. Patton:
 547 Language model pretraining on text-rich networks, 2023.

548 Thomas N. Kipf and Max Welling. Semi-supervised classification with graph convolutional net-
 549 works. In *ICLR*, 2017.

550 Chang Liu and Bo Wu. Evaluating large language models on graphs: Performance insights and
 551 comparative analysis, 2023.

552 Hao Liu, Jiarui Feng, Lecheng Kong, Ningyue Liang, Dacheng Tao, Yixin Chen, and Muhan
 553 Zhang. One for all: Towards training one graph model for all classification tasks. *arXiv preprint*
 554 *arXiv:2310.00149*, 2023.

555 Yuankai Luo, Veronika Thost, and Lei Shi. Transformers over directed acyclic graphs. In Alice
 556 Oh, Tristan Naumann, Amir Globerson, Kate Saenko, Moritz Hardt, and Sergey Levine (eds.),
 557 *NeurIPS*, 2023.

558 Andrew Kachites McCallum, Kamal Nigam, Jason Rennie, and Kristie Seymore. Automating the
 559 construction of internet portals with machine learning. *Information Retrieval*, 3:127–163, 2000.

560 Galkin Mikhail, Yuan Xinyu, Mostafa Hesham, Tang Jian, and Zhu Zhaocheng. Towards foundation
 561 models for knowledge graph reasoning. *ICLR*, 2024.

562 Yijian Qin, Xin Wang, Ziwei Zhang, and Wenwu Zhu. Disentangled representation learning with
 563 large language models for text-attributed graphs, 2024.

564 Zhixiang Su, Di Wang, Chunyan Miao, and Lizhen Cui. Multi-aspect explainable inductive relation
 565 prediction by sentence transformer, 2023.

566 Alon Talmor, Jonathan Herzig, Nicholas Lourie, and Jonathan Berant. Commonsenseqa: A question
 567 answering challenge targeting commonsense knowledge. In *NAACL*, pp. 4149–4158.

568 Yanchao Tan, Hang Lv, Xinyi Huang, Jiawei Zhang, Shiping Wang, and Carl Yang. Musegraph:
 569 Graph-oriented instruction tuning of large language models for generic graph mining. *CoRR*,
 570 abs/2403.04780, 2024.

571 Jiabin Tang, Yuhao Yang, Wei Wei, Lei Shi, Lixin Su, Suqi Cheng, Dawei Yin, and Chao Huang.
 572 Graphgpt: Graph instruction tuning for large language models, 2024.

573 Komal K. Teru, Etienne Denis, and William L. Hamilton. Inductive relation prediction by subgraph
 574 reasoning, 2020.

575 Petar Velickovic, Guillem Cucurull, Arantxa Casanova, Adriana Romero, Pietro Liò, and Yoshua
 576 Bengio. Graph attention networks. In *ICLR*, 2018.

577 Han Xie, Da Zheng, Jun Ma, Houyu Zhang, Vassilis N. Ioannidis, Xiang Song, Qing Ping, Sheng
 578 Wang, Carl Yang, Yi Xu, Belinda Zeng, and Trishul Chilimbi. Graph-aware language model
 579 pre-training on a large graph corpus can help multiple graph applications, 2023.

580 Yichong Xu, Chenguang Zhu, Shuohang Wang, Siqi Sun, Hao Cheng, Xiaodong Liu, Jianfeng
 581 Gao, Pengcheng He, Michael Zeng, and Xuedong Huang. Human parity on commonsenseqa:
 582 Augmenting self-attention with external attention. *arXiv preprint arXiv:2112.03254*, 2021.

583 Hao Yan, Chaozhuo Li, Ruosong Long, Chao Yan, Jianan Zhao, Wenwen Zhuang, Jun Yin, Peiyan
 584 Zhang, Weihao Han, Hao Sun, Weiwei Deng, Qi Zhang, Lichao Sun, Xing Xie, and Senzhang
 585 Wang. A comprehensive study on text-attributed graphs: Benchmarking and rethinking. In
 586 *NeurIPS*, 2023.

594 Junhan Yang, Zheng Liu, Shitao Xiao, Chaozhuo Li, Defu Lian, Sanjay Agrawal, Amit Singh,
 595 Guangzhong Sun, and Xing Xie. Graphformers: Gnn-nested transformers for representation
 596 learning on textual graph, 2023.

597 Zhilin Yang, William W. Cohen, and Ruslan Salakhutdinov. Revisiting semi-supervised learning
 598 with graph embeddings. In *Proceedings of the 33nd International Conference on Machine Learn-
 599 ing*, volume 48, pp. 40–48, 2016.

600 Liang Yao, Chengsheng Mao, and Yuan Luo. Kg-bert: Bert for knowledge graph completion, 2019.

601 Michihiro Yasunaga, Hongyu Ren, Antoine Bosselut, Percy Liang, and Jure Leskovec. Qa-gnn:
 602 Reasoning with language models and knowledge graphs for question answering. *NAACL*, 2021.

603 Hanwen Zha, Zhiyu Chen, and Xifeng Yan. Inductive relation prediction by bert, 2021.

604 Jianan Zhao, Meng Qu, Chaozhuo Li, Hao Yan, Qian Liu, Rui Li, Xing Xie, and Jian Tang. Learning
 605 on large-scale text-attributed graphs via variational inference. In *ICLR*, 2023.

606 Zhaocheng Zhu, Zuobai Zhang, Louis-Pascal Xhonneux, and Jian Tang. Neural bellman-ford net-
 607 works: A general graph neural network framework for link prediction, 2022.

608 Zhaocheng Zhu, Xinyu Yuan, Michael Galkin, Louis-Pascal Xhonneux, Ming Zhang, Maxime
 609 Gazeau, and Jian Tang. A* net: A scalable path-based reasoning approach for knowledge graphs.
 610 *Advances in Neural Information Processing Systems*, 36, 2024.

615 A EXPERIMENTAL DETAILS

616 **Architecture** All our models are based on Llama-3-8b, which utilizes a 32-layer Transformer,
 617 with message passing at layers 0, 4, 8, 12, 16, 20, 24, and 28, and node cross-attention at layers
 618 3, 7, 11, 15, 19, 23, 27, and 31. For the original LLaMA-3 layers, we employ LoRA with rank
 619 r and weight $\alpha = 2r$, while newly added layers are trained with full parameters. The LLM used
 620 for sentence encoding is LLM2Vec (BehnamGhader et al., 2024) model based on Llama-3-8b, is
 621 fine-tuned with Lora on its last layer. For ogbl-arxiv dataset, we use $r = 64$. For CSTAG datasets,
 622 we use $r = 4$. For all other datasets, we use $r = 32$. GNN in our model is implemented with torch
 623 geometric (Fey & Lenssen, 2019). Some parameters are loaded from pretrained LLM.

- 624 • For structure-aware Transformer Layers, we leverage the pretrained Llama-3-8B model as
 625 the backbone. As detailed in Section 3.1, we introduce new parameters through modifica-
 626 tions to positional encoding and attention masks. Additionally, for the <graph_node>
 627 token, we simply add an embedding to the existing layer. The newly added MPNN com-
 628 ponent is initialized randomly. We fine-tune the transformer parameters using the Low-
 629 Rank Adaptation (LoRA) method from the peft library. This approach freezes the original
 630 transformer layers and optimizes only the newly introduced low-rank layers. The MPNN
 631 parameters, on the other hand, are trained entirely from scratch.
- 632 • For the Graph-Text Cross-Attention layers in our paper, all parameters are initialized ran-
 633 domly and trained from scratch.
- 634 • For the GNN prediction modules, which are simple linear layers for generating outputs,
 635 parameters are initialized randomly and trained from scratch.
- 636 • Overall, most parameters are initialized from pretrained models and frozen. Only about
 637 10% of the parameters in the entire model are optimized.

638 **Training Process** All experiments are trained on A800 GPUs with one epoch. The optimizer is
 639 AdamW with learning rate=3e-5, weight decay=0.1. For node classification and csqa datasets, we
 640 ensemble the prediction of GNN and LLM. For link datasets, we use GNN output only. For graph
 641 level tasks and synthetic tasks, we use text output only. The entire model is trained end-to-end, with
 642 joint training of all components.

643 **Baselines** Baselines and experiments setting used in different works on combining GNN and LLM
 644 varies a lot. Therefore, we directly use the results reported by baseline works as shown in the
 645 maintext.

648 **B DATASET DETAILS**
649650 **B.1 DETAILS OF FB15K-237-IND DATASETS**
651652 Table 9: Statistics of FB15k-237-ind benchmark. (Teru et al., 2020)
653

		#links	#nodes	#links
v1	train	183	2000	5226
	ind-test	146	1500	2404
v2	train	203	3000	12085
	ind-test	176	2000	5092
v3	train	218	4000	22397
	ind-test	187	3000	9137
v4	train	222	5000	33916
	ind-test	204	3500	14554

666 The statistics of the FB15k-237-ind is in Table 9. To generate the text attributes of the datasets,
667 we first map Freebase objects to wikidata¹, and then used the detailed texts from the wikiKGv2-
668 90m dataset in OGB-LSC (Hu et al., 2021) as the textual representations for each node. Like other
669 KG completion work on GNN, we also added reverse relation for each relation and label them as
670 “[reverse] xxx”.

671 The total graph is too large to input the GNN, so like previous work we sample a subgraph. For
672 training set, we first sample random 50 negative samples by perturb the head or tails of a triple and
673 then sample the 3-hop neighbors of these nodes. Then we reduce the subgraph size with limiting the
674 maximal number of nodes is 500.

675 An example of our dataset:

676 The input question:

677 The Adventures of Tintin (2011 film directed by Steven Spielberg)
678 -/film/film/production_companies → ?. The graph: <graph_start><node><node>...<node><graph_end>.

679 The node text features in the graph:

680 `{“title”: “Jane Krakowski”, “desc”: “American actress”, “dist to head”: 6}`
681 `{“title”: “Shochiku”, “desc”: “Japanese movie studio and production company for kabuki.”, “dist to head”: 3}`
682 `{“title”: “Erin Brockovich”, “desc”: “2000 biographical movie by Steven Soderbergh”, “dist to head”: 2}`
683 ...

684 The relation text features:

685 `{“title”: “/film/film/runtime/film/film_cut/film_release_region”}`
686 `{“title”: “[reverse] /music/record_label/artist”}`
687 ...

688 **B.2 DETAILS OF CSTAG DATASETS**
689

690 CSTAG datasets, including children, history, computers. photo, sport, are provided by Yan et al.
691 (2023). We conduct node classification tasks on them. Their statistics are shown in Table 10. We
692 directly use the node text provided by the dataset.

694 **B.3 DETAILS OF CITATION GRAPHS**
695

696 We use citation graphs ogbn-arxiv (Hu et al., 2020) and cora (Liu et al., 2023) and classify nodes on
697 them. Their statistics are shown in Table 11. For ogbn-arxiv, we directly use official split. For node
698 text, we use paper title and abstract. We also add label of non-target nodes in training set to input
699 node text. The edge text are “cite” or “cited”.
700

701 ¹There are some tools to convert FB to wikidata, like <https://github.com/happen2me/freebase-wikidata-convert?tab=readme-ov-file>

702
703
704 Table 10: Statistics of CSTAG datasets.
705
706
707
708
709
710

Dataset	#Nodes	#Edges	#Class	Split	Ratio	Metric	text length
Children	76,875	1,554,578	24	Random	60/20/20	Acc	256
History	41,551	358,574	12	Random	60/20/20	Acc	256
Computers	87,229	721,081	10	Time	72/17/11	Acc	256
Photo	48,362	500,928	12	Time	60/20/20	Acc	512
Sports	173,055	1,773,500	13	Random	20/10/70	F1	64

711
712 Table 11: Statistics of citation datasets.
713
714

Dataset	#Nodes	#Edges	#Class	Split	Ratio	Metric	text length
ogbn-arxiv	169,343	1,166,243	40	Time	54/18/28	Acc	256
Cora	2,807	5,429	7	Random	10/10/80	Acc	256

718
719 B.4 DETAILS OF COMMON SENSE QUESTION ANSWERING DATASET.720
721 Common Sense Question Answering dataset (Talmor et al.) is a dataset answering common sense
722 questions based on knowledge graph. Each question is a 5-way multiple choice task that requires
723 reasoning with commonsense knowledge. The dataset contains 12,102 questions. The split is fixed.
724 The test set of CommonsenseQA is not publicly available, and model predictions can only be eval-
725 uated once every two weeks. So we report results on the in-house (IH) data splits used in Yasunaga
726 et al. (2021).727
728 B.5 DETAILS OF GRAPH PROPERTY PREDICTION DATASET.729 We use ogbg-code2 (Hu et al., 2020), a dataset containing 158,100 code graphs with each graph
730 containing 125.2 nodes and 124.2 edges on average. The task is to predict the function name of the
731 code represented by the graph. We use node type in compiler and node attribute (values of constants)
732 as the node feature.733
734
735
736
737
738
739
740
741
742
743
744
745
746
747
748
749
750
751
752
753
754
755